Simulation of a Single Vertical U-Tube Ground Heat Exchanger in an Infinite Medium

Steve P. Rottmayer
Student Member ASHRAE

William A. Beckman, Ph.D.

John W. Mitchell, Ph.D., P.E.
Fellow ASHRAE

ABSTRACT

Geothermal (ground-source) heat pumps (GHPs) are an efficient alternative to conventional methods of conditioning buildings. However, GHP systems can have relatively high installation costs because of the ground heat exchanger. Proper sizing of the exchanger is critical to performance. Vertical U-tube heat exchangers are commonly used as the ground heat exchanger, but the design and determination of the operating performance is difficult because of the unique heat transfer situation. This paper proposes a U-tube heat exchanger model based on finite-difference methods that can be used in system design and annual performance simulations.

INTRODUCTION

Ground-source or geothermal heat pumps use the ground as a heat sink or source. The temperature of the ground becomes relatively constant with depth and is closer than the ambient air to the temperature desired for human comfort. This nearly constant temperature results in a high level of heat pump performance even in extreme climates. Many public utilities and energy service companies (both independent and utility affiliates) endorse the use of geothermal heat pumps and are currently active in persuading the heating, ventilating, and air-conditioning (HVAC) industry and customers to increase the number of units installed.

Ground-source heat pump systems often employ a closed-loop ground-coupled heat exchanger consisting of either vertical or horizontal tubes. Vertical U-tube heat exchangers can be expensive but are often used instead of horizontal units because they are require less surface area. The U-tube is usually a plastic tube ¾-in. to 1¼ in. (19 to 31.7 mm) in diameter with a U-bend in the middle that reverses the direction of fluid flow, as shown in Figure 1. The U-tube is inserted in a vertical borehole in the ground, and the borehole is filled with backfill or grout. The heat exchange fluid travels through the tubes and exchanges heat with the ground. It is difficult to accurately represent the unique heat transfer conditions of this configuration, and many models (e.g., Muraya 1995) have been created to simulate U-tube operation. In the past, numerical models have required a significant amount of computer runtime, and, consequently, most of today's models still rely on analytical methods referred to as the "line source theory" (Ingersoll et al. 1954) and the "cylindrical source theory" (Carslaw and Jaeger 1946).

This paper proposes a finite-difference model for the simulation of a vertical U-tube ground heat exchanger that can enhance existing design tools by providing a comparative solution. The heat exchanger is modeled using a finite-difference approach to the three-dimensional transient conductive heat transfer in the ground. The program allows the user to change the

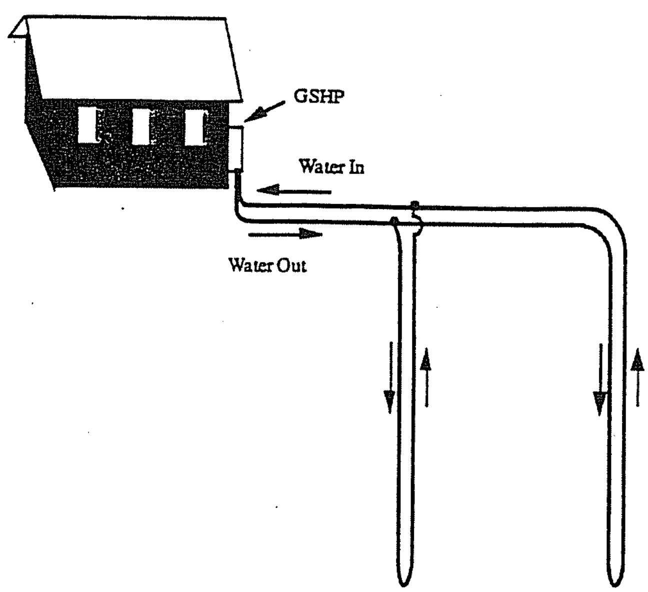

Figure 1 GHP with two vertical U-tube heat exchangers in parallel.

Steve P. Rottmayer is a research assistant and **William A. Beckman** and **John W. Mitchell** are professors in the Department of Mechanical Engineering at the University of Wisconsin, Madison.

borehole depth, bore diameter, pipe diameter, simulation duration, fluid flow rate, as well as the properties and temperature of the ground, grout, and inlet fluid. The soil properties are assumed to be constant over the period of the simulation. Results obtained from the simulations are compared with solutions from other numerical models.

MODEL DEVELOPMENT

The thermal system of a U-tube heat exchanger consists of the heat transfer fluid, U-tubes, borehole grout, and the surrounding ground formation. The volume of ground that is affected by the U-tube exchanger is referred to as the ground storage volume. For modeling purposes, the ground storage volume can be considered a cylinder with a height equal to the depth of the borehole. The radius of the cylinder is large enough to ensure that the soil at the edge is not significantly affected by the U-tubes at its center; this is referred to as the *farfield radius*. The temperature of the ground at the farfield radius is a function of depth determined using the relationship of Kusuda and Archenbach (1965).

The cylinder is divided axially into sections, with each section representing the ground at a specific depth, as shown in Figure 2. The heat transfer is symmetrical about a vertical plane passing through the center of the tubes. Consequently, it is only necessary to model half of the ground storage volume and its associated tubes, fluid, and grout. The model developed allows heat transfer in the ground to occur radially and circumferentially, but not axially. The assumption of no axial conduction is justified because of the large distances between axial nodes relative to the temperature difference. A two-dimensional cylindrical grid represents the fluid, tubes, grout, and soil at one axial section. The reason behind this choice of grid geometry is to create a circular grid outside the borehole that allows the nodal spacing to increase in the radial direction, which minimizes the total number of nodes required.

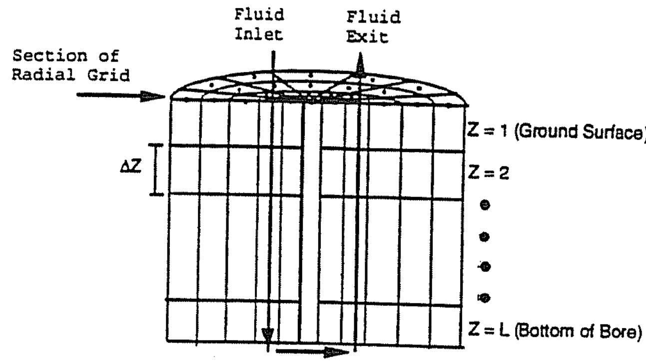

Figure 2 *Combination of cylindrical grids to provide a three-dimensional model of a U-tube.*

It is difficult to create a general finite-difference formulation for the two tubes that are encased in grout and buried in the ground. For simplicity in modeling, the circular tubes are approximated as noncircular sections, as shown in Figure 3. The

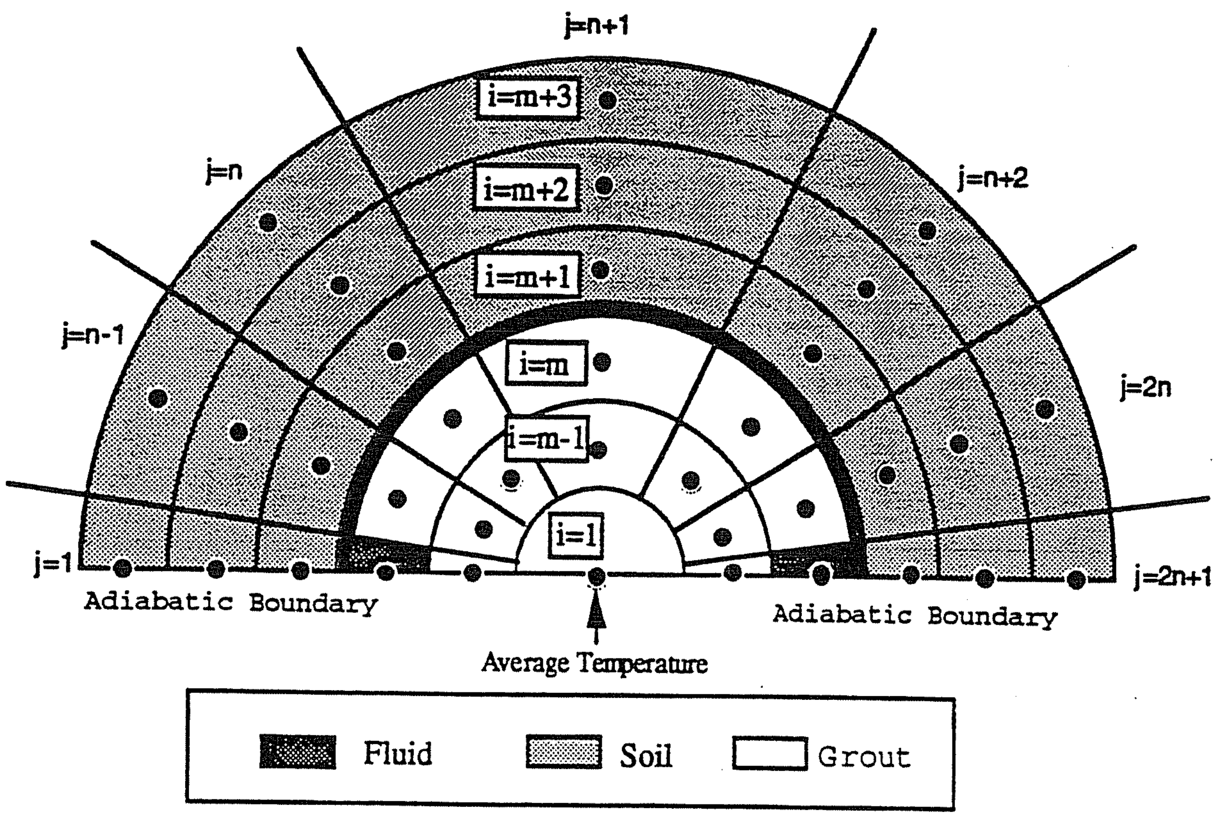

Figure 3 *Cylindrical finite-difference grid used to calculate the heat transfer at one depth. For typical configurations,* m = n = *3 as shown.*

node positions are represented by the variables i in the radial direction, j in the azimuth direction, z in the vertical direction, and k in time. The variables n and m are integers and their importance is explained later (the values of m and n are 3 in Figure 3). For the results presented in this paper and as shown in Figure 3, the radial position of the tubes is at the edge of the borehole ($i = m$). However, the model allows the tubes to be placed at other radial positions and is only restricted in that the spacing between the centers of the tubes must be greater than three diameters. The cylindrical grids are then used at each axial section to create the three-dimensional model shown in Figure 2. The fluid enters at the surface ($z = 1$), travels through to the bottom of the grid ($z = L$), back up the return tube, and exits again at the top ($z = 1$).

Figure 4 shows the resistance network for the soil and the grout nodes. The special nodes at $j = n + 1$ and the nodes adjacent to the U-tube are discussed later. The resistance between nodes in the soil in the radial direction is given by

$$R(i,j) = \frac{ln\left(\frac{r(i+1)}{r(i)}\right)}{k_s \cdot \Delta\theta \cdot \Delta Z} \tag{1}$$

and the resistance between the nodes in the soil in the circumferential direction is given by

$$R(i,j+1) = \frac{\Delta\theta \cdot r(i)}{k_s \cdot \Delta Z \cdot (r_m(i) - r_m(i-1))}. \tag{2}$$

The resistance equations for the grout material are identical to those for the soil, with the soil conductivity (k_s) replaced with the grout conductivity (k_g). Equation 3 is used to calculate the resistance between the nodes at the grout-to-soil interface, where r_m is the radius halfway between the nodes:

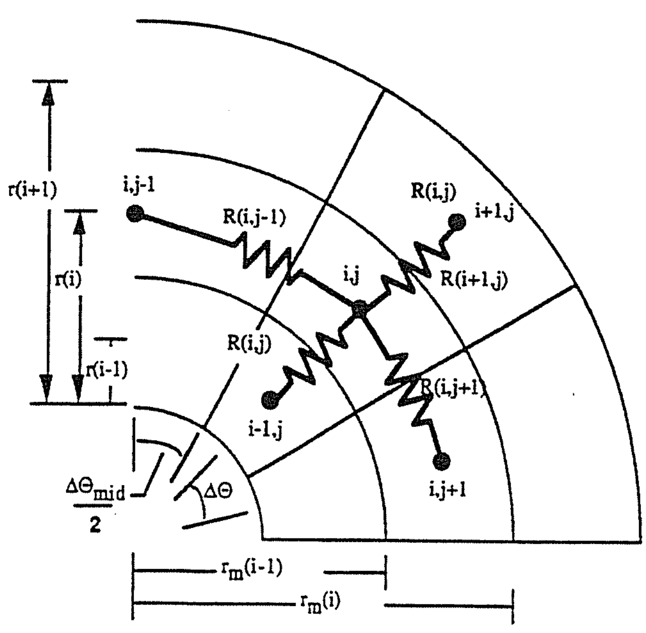

Figure 4 *Resistance network for cylindrical mesh.*

$$R(m,j) = R_g + R_s \tag{3}$$

where

$$R_g = \frac{\ell n\left(\frac{r_m(m)}{r(m)}\right)}{k_g \cdot \Delta\theta \cdot \Delta Z} \tag{3a}$$

and

$$R_s = \frac{\ell n\left(\frac{r(m+1)}{r_m(m)}\right)}{k_s \cdot \Delta\theta \cdot \Delta Z}. \tag{3b}$$

An explicit (Euler) finite-difference formulation is used to represent the energy balance on a soil node, as given by

$$\begin{aligned}(\rho c V(i))_s \frac{(T(i,j,z,k+1) - T(i,j,z,k))}{\Delta t_2} &= \frac{(T(i-1,j,z,k) - T(i,j,z,k))}{R(i-1,j)} \\ &+ \frac{(T(i+1,j,z,k) - T(i,j,z,k))}{R(i,j)} \\ &+ \frac{(T(i,j-1,z,k) - T(i,j,z,k))}{R(i,j-1)} \\ &+ \frac{(T(i,j+1,z,k) - T(i,j,z,k))}{R(i,j+1)}.\end{aligned} \tag{4}$$

Consistent with the development of the Lund model (Hellstrom 1991), the capacitance of the tube wall and grout is neglected. The capacitance of these elements is small relative to that of the ground and inclusion of these capacitances would require very small time steps. The thermal energy change of the grout over a year is on the order of 0.5% of the total heat flow, and thus the wall and grout capacitances are not significant in annual simulations. However, neglecting the pipe wall and grout capacitances might affect the short time response and could be readily included. The grout node temperatures are calculated using Equation 5.

$$\begin{aligned}0 &= \frac{T(i-1,j,z,k) - T(i,j,z,k+1)}{R(i-1,j)} \\ &+ \frac{T(i+1,j,z,k) - T(i,j,z,k)}{R(i,j)} \\ &+ \frac{T(i,j+1,z,k) - T(i,j,z,k)}{R(i,j+1)} \\ &+ \frac{T(i,j-1,z,k) - T(i,j,z,k)}{R(i,j-1)}.\end{aligned} \tag{5}$$

The radial spacing, ΔR, and the angular spacing, $\Delta\theta$, are chosen such that the perimeter of the circular pipes and the cylindrical grid sections that represent the pipes are equal. Since $\Delta\theta$ is a function of the tube size, it will not necessarily be an integer divisor of 180 degrees. To account for this, the angular spacing between nodes is taken to be $\Delta\theta$ except at $j = n + 1$, where the angular separation is $(\Delta\theta/2 + \Delta\theta_{mid}/2)$. Equations 1 and 3 are then modified by replacing $\Delta\theta$ with $\Delta\theta_{mid}$. Equation 2 requires the replacement of $\Delta\theta$ with $(\Delta\theta/2 - \Delta\theta_{mid}/2)$, and Equation 4 is

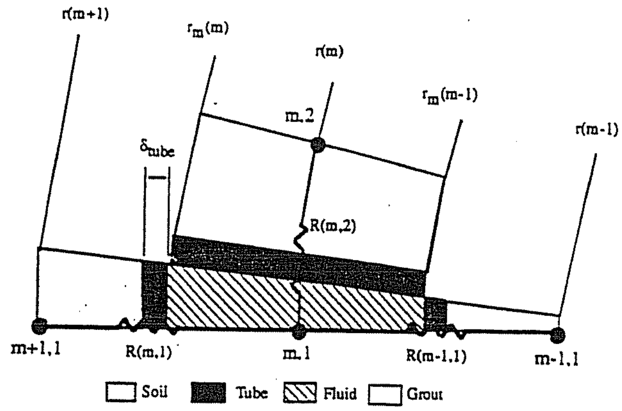

Figure 5 *Resistance network of noncircular tubes.*

modified by calculating the volume $V(i)$ with $\Delta\theta_{mid}$ instead of $\Delta\theta$. The nodes along the adiabatic boundary ($j = 1$ and $j = 2n + 1$) use $\Delta\theta$ spacing but are only half the volume of the other nodes.

As indicated, the pipe tubes in the finite-difference mesh are not circular but are approximated by noncircular sections in the grid. The fluid-to-ground thermal resistance is calculated with three combined resistances, $R(m-1,1)$, $R(m,1)$, and $R(m,2)$, as shown in Figure 5. Each combined resistance consists of the resistance from the fluid to the tube wall, the tube resistance, and the resistance of the soil or grout. Equations 6 through 8 are used to determine $R(m-1,1)$, $R(m,1)$, and $R(m,2)$. Since ΔR and $\Delta\theta$ are calculated so that the inside perimeters of the noncircular and circular pipe tubes are equal, the cross-sectional (flow) areas are not equal. Using the flow area calculated with the noncircular grid would produce a velocity different from the actual velocity. In the model, the fluid velocity and transit time for the noncircular tube are set to be the same as for the actual circular tube.

$$R(m-1,1) = R(m-1,1)_f + R(m-1,1)_t + R(m-1,1)_g \quad (6)$$

$$R(m-1,1)_f = \frac{1}{h\Delta Z\frac{\Delta\theta}{2}r_m(m-1)} \quad (6a)$$

$$R(m-1,1)_t = \frac{\ln(r_m(m-1)/(r_m(m-1)-\delta_t))}{\left(\frac{\Delta\theta}{2}\right)k_t\Delta Z} \quad (6b)$$

$$R(m-1,1)_g = \frac{\ln((r_m(m-1)-\delta_t)/r(m))}{\left(\frac{\Delta\theta}{2}\right)k_g\Delta Z} \quad (6c)$$

$$R(m,1) = R(m,1)_f + R(m,1)_t + R(m,1)_s \quad (7)$$

$$R(m,1)_f = \frac{1}{h\Delta Z\frac{\Delta\theta}{2}r_m(m)} \quad (7a)$$

$$R(m,1)_t = \frac{\ln(r_m(m)/(r_m(m)+\delta_t))}{\left(\frac{\Delta\theta}{2}\right)k_t\Delta Z} \quad (7b)$$

$$R(m,1)_s = \frac{\ln((r(m-1)-\delta_t)/r_m(m))}{\left(\frac{\Delta\theta}{2}\right)k_s\Delta Z} \quad (7c)$$

$$R(m,2) = R(m,2)_f + R(m,2)_t + R(m,2)_g \quad (8)$$

$$R(m,2)_f = \frac{1}{h\Delta Z(r_m(m)-r_m(m-1))} \quad (8a)$$

$$R(m,2)_t = \frac{\delta_t}{k_t\Delta Z(r_m(m)-r_m(m-1))} \quad (8b)$$

$$R(m,2)_g = \frac{\left(r(m)\left(\frac{\Delta\theta}{2}\right)-\delta_t\right)}{k_g\Delta Z(r_m(m)-r_m(m-1))} \quad (8c)$$

The temperature of the node in the center of the mesh ($i = 1$) is determined from the resistances between the center node and its adjacent nodes as determined from Equations 9 and 10. Using these resistances, an energy balance on the center node will result in a central node temperature that is equal to the average temperature of its surrounding nodes.

$$\pi \cdot r_{half}^2 = \pi(r_m(1)^2 - r_{half}^2) \quad (9)$$

$$R(1,j) = \frac{\ln\left(\frac{r(2)}{r_{half}}\right)}{k_g \cdot \Delta\theta \cdot \Delta Z} \quad (10)$$

The equations for the heat transfer from the tubes to the ground are determined from an energy balance on the fluid. For a fluid flowing downward through tubes located at positions given by indices m and j, the energy balance is expressed in finite-difference form by Equations 11 and 12:

$$(\rho Vc)_f\frac{(T(m,j,z,k-1)-T(m,j,z,k))}{\Delta t_1} = \dot{m}c(T(m,j,z-1,k)-T(m,j,z,k)) - Q_{out} \quad (11)$$

where the axial position is indicated by the index z and time by the index k.

$$Q_{out} = \frac{T(m,j,z,k)-T(m-1,j,z,k)}{R(m-1,1)} + \frac{T(m,j,z,k)-T(m+1,j,z,k)}{R(m,1)} + \frac{T(m,j,z,k)-T(m,j+1,z,k)}{R(m,2)} \quad (12)$$

Equations 1 through 12 have been combined into a transient model for the ground-source heat exchanger. The time required to perform calculations is reduced by minimizing the number of nodes and splitting the system into two time domains.

The number of nodes in the system is dependent on the nodal spacing. The number of nodes in the circumferential and axial directions depends on the system geometry. Currently, the distance between axial nodes is 10 ft (3 m), but this distance could be increased or decreased depending on the level of accuracy desired. The radial spacing for the tubes and the nodes close to the tubes depends on the U-tube inner diameter. The node spacing is chosen to be small close to the tubes because the temperature gradients are large. As the radial distance from the tubes increases, the temperature gradients decrease, making it possible to increase the radial spacing without loss in accuracy.

Two time steps are used, one for the fluid transport (Δt_1) and one for the heat transfer to the ground (Δt_2). The system was split into these two domains because the critical time step for the soil is often an order of magnitude greater than the critical time step for the fluid and allows for much larger time steps. The maximum value of Δt_1 is given by the time it takes the fluid to travel through one axial section:

$$\Delta t_1 \leq \frac{\Delta Z}{Vel_f}. \tag{13}$$

The maximum value of Δt_2 is found for each node by dividing the sum of the thermal capacity of the node by the sum of its surrounding thermal resistances. The maximum value of Δt_2 is the smallest value of these critical time steps:

$$\Delta t_2 = \text{minimum}(\Delta t_i) = \text{minimum}\left(\frac{\text{mass}_i c_i}{\Sigma 1/R_i}\right). \tag{14}$$

Using two time steps decreased the simulation time by about 80% over simulations in which the time steps were the same for both fluid and ground.

For the U-tube geometry specified in Table 1 the number of nodes radially, circumferentially, and axially were 17, 7, and 20, respectively, and the time steps for the fluid and ground were 20 seconds and 3 minutes, respectively. The model was able to complete an annual simulation in approximately half an hour on a 166-Mhz computer.

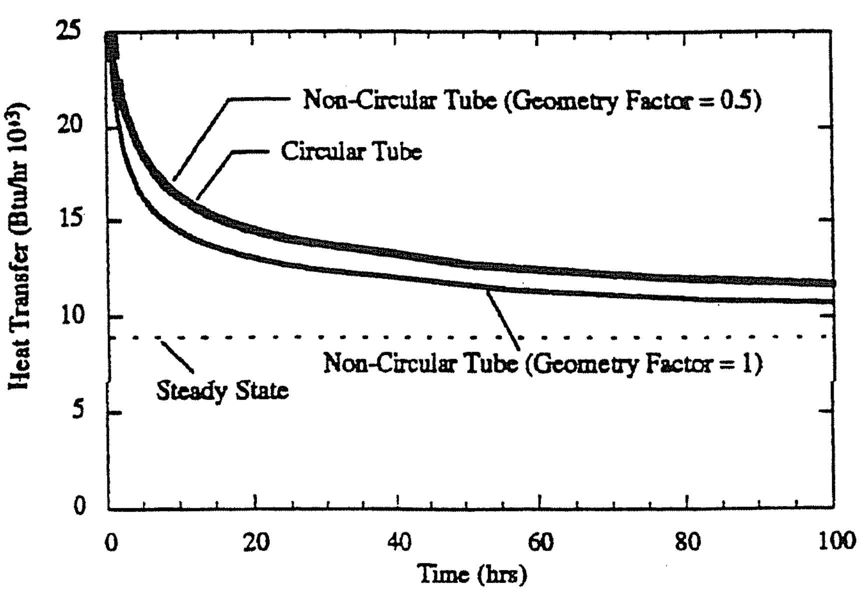

Figure 6 Comparison of a circular and a noncircular tube (0-100 hours).

TABLE 1
Single-Tube Finite-Difference Comparison

Fluid Inlet Temp.	100°F (37.7°C)	ρ_s	131 lb/ft³
Farfield Radius	10 ft (3 m)	c_s	0.2 Btu/lbm·°F
Farfield Temperature	0°F (−17.7°C)	k_g	0.75 Btu/h·ft·°F
Inner Tube Diameter	1.5 in. (3.8 cm)	Depth	200 ft (60.9 m)
c_f	1012 Btu/lbm·°F	k_{tube}	0.226 Btu/h·ft·°F
k_s	0.75 Btu/h·ft·°F	Flow Rate	3 gpm

VALIDATION OF THE MODEL

The model was first verified by comparing results with a finite-difference model of a single circular tube. The cylindrical grid shown in Figure 3 was altered to allow calculation of the heat transfer from a single-tube heat exchanger. The node that was originally used as the return tube of the U-tube was reprogrammed to be ground material. Therefore, the model would represent a single tube slightly off center (4 in. [10.1 cm] from the center of the grid). Soil and fluid properties were taken from the literature as typical values for heat pump applications. The grout properties were set equal to those of the surrounding ground for the validation tests. The model was run with the conditions shown in Table 1. For comparison, the steady-state solution was also calculated using heat exchanger effectiveness NTU relations (Incropera and DeWitt 1990). A large value of fluid-specific heat (10^{12}) was used to maintain a constant fluid temperature with depth.

The results of these simulations are shown in Figure 6 along with the steady-state solution obtained analytically. The heat transfer from the different models is plotted as a function of time. It can be seen that the results for the noncircular tube (labeled as geometry factor = 1) are below the circular tube solution by about 5%. The reason for this difference was determined to be due to the effect of the different shapes of the tubes on the heat transfer. The thermal resistances near the noncircular tube are significantly different from those near the circular tube. Although the noncircular model provides relatively good agreement, an empirically determined geometric factor is used to improve the model.

The soil and grout components of the fluid to ground resistances (Equations 6c, 7c, and 8c) are multiplied by a geometric factor to account for the effect of the noncircular geometry (Figure 5). The value of the factor was determined so that the heat transfer for the noncircular geometry gave the same steady-state heat transfer as that for a circular tube. The geometric factor was applied to only the soil and grout components because their thermal resistance is relatively more constant than the convection resistance (Equations 6a, 7a, and 8a) or the tube resistance (Equations 6b, 7b, and 8b). This is important because, in order to be useful, the geometric factor needs to be independent of the configuration and material properties of the system. The geometric factor was first determined by matching the heat transfer from the noncircular tube with that of a circular tube under the conditions listed in Table 1. For this case the geometric factor should be 0.5. The simulation for a geometric factor of 0.5 is also shown in Figure 6, and the computed heat transfer using this factor is virtually identical to that for the circular tube.

The steady-state temperature contours for the simulations of the circular tubes and the noncircular tubes with the geometric factor applied were also compared. As shown in Figure 7, there is excellent agreement between the two models.

It is probable that the geometric factor is dependent on four variables: ΔR, $\Delta\theta$, k_s, and k_g. After an appropriate geometric factor was determined for the initial case, several more simulations were run to estimate its dependency on these variables. It was found that the geometric factor was mainly dependent on the properties of the materials (k_s and k_g) and showed little effect of the geometry of the system. The average value from simulations for the conditions shown in Table 2 was determined to be 0.38. Without the geometric factor, the differences in heat flow are within 8%. Using the average geometric factor value of 0.38, the heat flow from the noncircular tube nodes was within 3% of that for the circular tube for all cases.

TABLE 2
Values Used to Determine the Largest and Smallest Geometric Factors

Parameter	ΔR	$\Delta\theta$	k_s	k_g
Small Value	0.033 ft	0.13 radians	0.2 Btu/h·ft·°F	0.2 Btu/h·ft·°F
Large Value	0.13 ft	0.52 radians	1.5 Btu/h·ft·°F	1.5 Btu/h·ft·°F

The accuracy of the noncircular tube model in simulating the two-dimensional heat transfer from two tubes was evaluated. The finite-difference model with noncircular tubes was run to steady state under the conditions shown in Table 3. The fluid temperatures at the ground surface ($z = 1$) were determined and then used as constant-temperature boundary conditions in an established finite-element heat transfer program (FEHT, Klein et al. 1997). The steady-state temperature distributions from these two models were compared. The temperature contours of the ground surrounding the U-tube were compared. As shown in Figure 8, there is good agreement between the temperature contours for the two cases.

The results from the finite-difference model were also compared to those from the line source model created at a Swedish university (Hellstrom 1991). The comparison is based on the specifications given in Table 4. These conditions are similar to those at Fort Polk, Louisiana, for which the performance has been determined (Thornton et al. 1996).

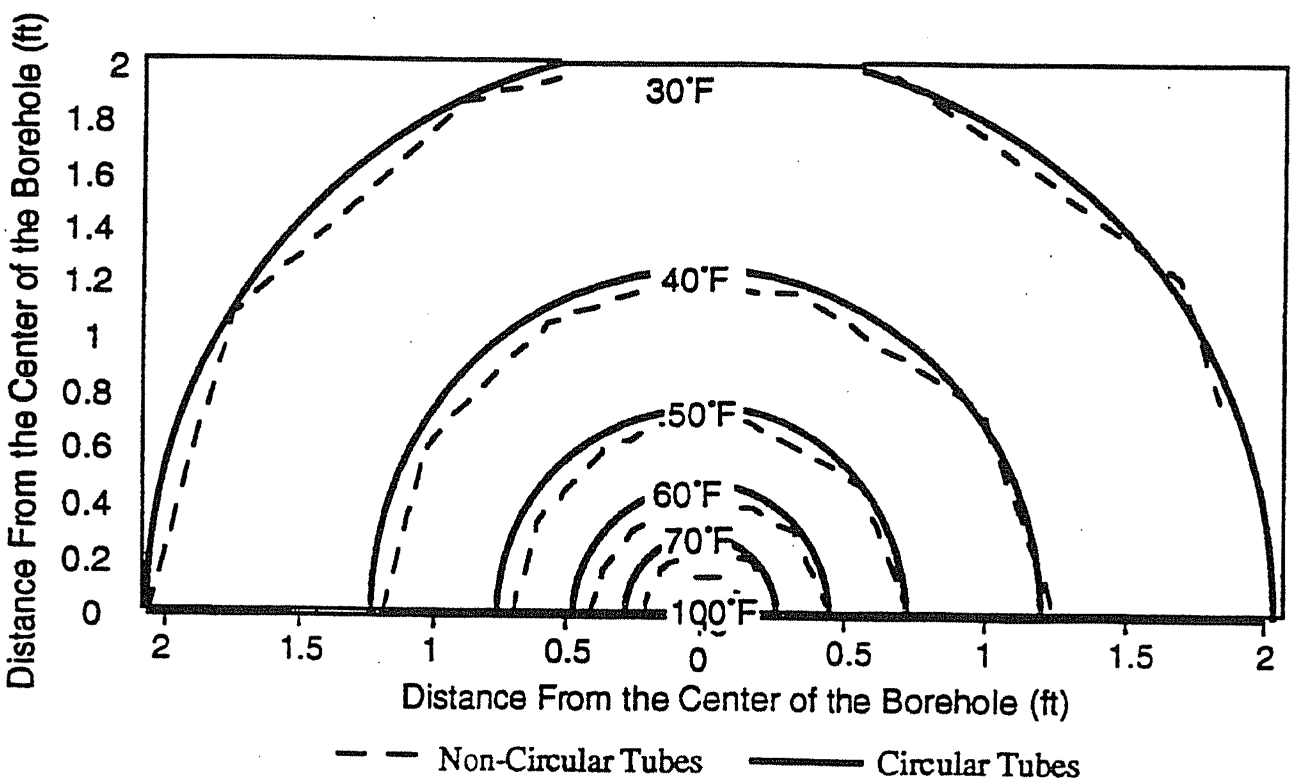

Figure 7 Comparison of one circular and one noncircular tube (2 ft).

TABLE 3
Two-Tube Finite Element Comparison

ρ_s	131 lb/ft^3	Fluid Inlet Temp.	100°F (37.7°C)
c_s	0.2 Btu/lbm·°F	Farfield Radius	8 ft (2.4 m)
k_g	0.75 Btu/h·ft·°F	Farfield Temperature	0°F (−17.7°C)
k_{tube}	0.75 Btu/h·ft·°F	Inside Tube Diameter	1.3 in. (3.3 cm)
flow rate	1.5 gpm	c_f	0.998 Btu/ lbm·°F
k_s	0.75 Btu/h·ft·°F		

TABLE 4
Parameters Used to Compare with the Hellstrom (1991) Model

T_{inlet}	100°F (37.7°C)	t_{shift}	32 days
T_{mean}	69°F (20.5°C)	c_f	0.998 Btu/ lbm·°F
Amplitude	17°F (−8.3°C)	mu_f	2.07 lbm/ft·h
k_s	1.4 Btu/h·ft·°F	k_f	0.353 Btu/ h·ft·°F
c_s	0.2 Btu/lbm·°F	U-Tube Spacing	3 in. (7.6 cm)
ρ_s	200 lbm/ft^3	Borehole Depth	200 ft (60.9 m)
k_g	1.4 Btu/h·ft·°F	Inner Tube Diameter	1.1 in. (2.7 cm)
k_t	0.2427 Btu/ h·ft·°F	Outer Tube Diameter	1.3 in. (3.3 cm)
ρ_f	62.4 lbm/ft^3	Flow Rate	1.5 gpm
Geometry Factor	0.38		

The Swedish model determines the total heat transfer from the U-tubes in two calculations. The first calculation determines the heat transfer to the ground near the tubes and is referred to as the "local" process. The local problem is solved in two steps. The first step determines an effective fluid to borehole resistance and then applies heat flux step pulses to obtain an average borehole temperature. A finite-difference mesh is then employed beyond the borehole wall to calculate the heat transfer to the local storage volume. The volume of ground considered in this local process is specified by the user. The second calculation determines the heat rejected from the local ground volume to the surrounding ground. The volume of the ground surrounding the local ground volume is determined by the model based on the ground heat exchanger configuration and the time of the simulation. The far edge of this volume is considered an adiabatic boundary.

The Swedish model enables the user to insulate the top and side of the local storage volume, and this feature was utilized for the first comparison between the two models. The size of the local storage volume for both the Swedish and the finite-difference models was set to equal 31,673 ft^3 (896.8 m^3) (a cylinder with a radius of approximately 7.1 feet [2.1 m] and a height of 200 feet [60.9 m]) and the edges of both boundaries were insulated.

The two models were run with the conditions shown in Table 4, and comparisons were made between the fluid exit temperature and the heat transferred to the ground. After a one-year simulation, the fluid exit temperature of the Swedish model was 98.2°F (36.7°C) and the finite-difference model provided a temperature of 98.6°F (37°C). The finite-difference model showed that the U-tubes transferred 33.7 MBtu of heat to the ground and the Swedish model provided slightly different answers, depending on how the calculation was performed. If the heat transfer was determined by the temperature rise in the

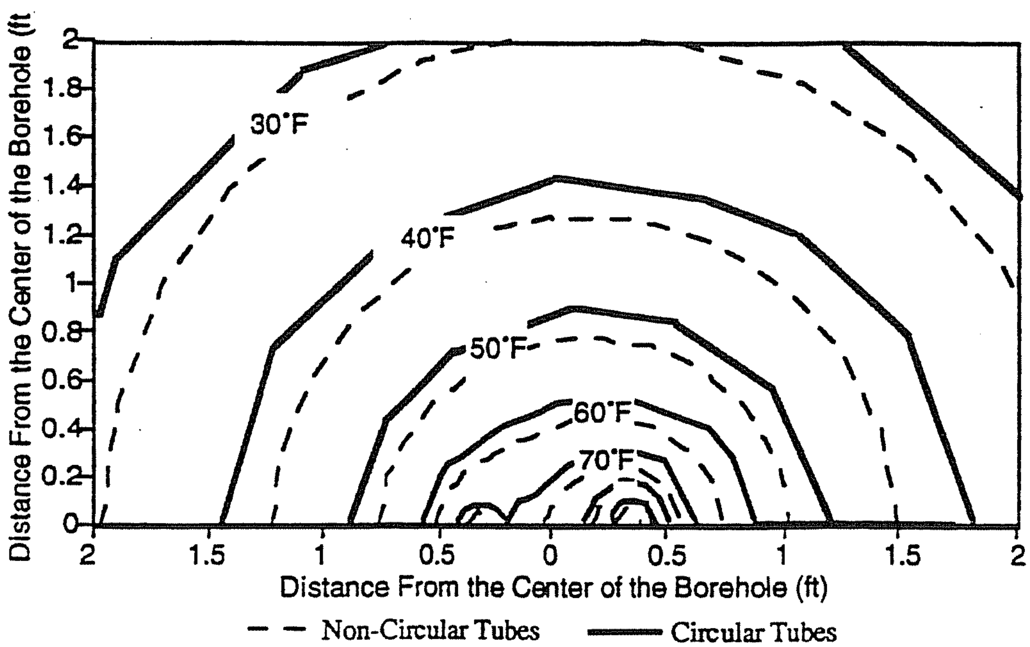

Figure 8 Comparison of two circular and two noncircular tubes (2 ft).

ground, the model showed that 32.8 MBtu were transferred to the ground. If an energy balance on the fluid nodes was integrated with time, the model provided an answer of 35.1 MBtu. These values are different from the finite-difference model by 2.6% and 4.1%, respectively. The main reason for this difference appears to be the difference in the manner that heat transfer from the bottom of the local storage volume is calculated. The outlet temperature of the fluid over time from the two models was in excellent agreement (within 1°F [0.5°C]).

A second comparison between the two models was made using the conditions shown in Table 4 with the insulation along the side of both storage volumes removed to allow heat transfer to the surrounding ground. The finite-difference model employed a constant-temperature boundary at 20 feet (6 m) from the U-tubes, while the Swedish model employed the adiabatic boundary as described previously. The results of this simulation also provided nearly identical results, with the Swedish model and the finite-difference model showing fluid exit temperatures of 90.8°F (32.6°C) and 90.5°F (32.5°C), respectively. The agreement in the long-term response establishes confidence in the current finite-difference model with noncircular tubes.

RESULTS AND CONCLUSION

This paper presented a finite-difference model that simulates the unique heat transfer conditions present in a U-tube heat exchanger. A geometric factor was introduced to account for the noncircular geometry used to represent the pipes in the borehole. The model has been validated for simple conditions and can be extended to include realistic conditions such as those for varying ground properties with depth and interference from other boreholes. Improvements such as these will increase the usefulness of the model to industry. The model was compared to an existing model used to estimate the performance of ground-coupled heat exchangers and showed good agreement.

The finite-difference approach is fundamental and provides flexibility in modeling complex situations for which the line source and cylindrical source models are less applicable. The accuracy and speed are dependent on the geometry of the system. Annual simulations for typical U-tube configurations can be performed in about 30 minutes on a 166-Mhz computer.

NOMENCLATURE

c = specific heat
δ = thickness
Δt_2 = time step for the soil nodes
Δt_1 = time step for the fluid nodes
ΔR = radial distance between nodes
$\Delta\theta$ = angular dimension of a node
$\Delta\theta_{mid}$ = angular dimension between nodes
h = fluid-to-tube heat transfer coefficient
k = thermal conductivity of soil
m = radial position of the tubes and edge of grout
n = number of multiples of $\Delta\theta$ contained in 90°
ρ = density
Q_{out} = heat transfer from tubes
r = radius at node
r_m = radius halfway between nodes
R = resistance
r_{half} = radius between the center and second nodes
T = temperature
V = volume
Vel = velocity
ΔZ = axial distance between nodes

Array Variables

i = radial position of the nodes
j = circumferential position of the nodes
k = time step
z = axial position of the nodes

Subscripts

f = fluid
g = grout
s = soil
t = tube

REFERENCES

Carslaw, H.S., and J.C. Jaeger. 1946. *Conduction of heat in solids*. Oxford, U.K.: Claremore Press.

Cengel, Y.A., and M.A. Boles. 1989. *Thermodynamics—An engineering approach*. New York: McGraw-Hill.

Ferziger, J.H. 1981. *Numerical methods for engineering application*. New York: John Wiley and Sons.

Giardina, J. 1994. Evaluation of ground coupled heat pumps for the state of Wisconsin. M.S. thesis, University of Wisconsin, Madison.

Hellstrom, G. 1991. Ground heat storage: Thermal analyses of duct storage systems. Lund, Sweden: University of Lund.

Incropera, F.P., and D.P. DeWitt. 1990. *Introduction to heat transfer*. New York: John Wiley and Sons.

Ingersoll, L.R., O.J. Zobel, and A.C. Ingersoll. 1954. *Heat conduction with engineering, geological, and other applications*. New York: McGraw-Hill.

Klein, S.A., et al. 1996. TRNSYS—A transient system simulation program, version 14.1. Madison: Solar Energy Laboratory, University of Wisconsin.

Klein, S.A., et al. 1988-1997. FEHT—A finite element heat transfer program. Madison: Solar Energy Laboratory, University of Wisconsin.

Kusuda, T., and P.R. Archenbach. 1965. Earth temperature and thermal diffusivity at selected stations in the United States. *ASHRAE Transactions* 71(1).

Muraya, N.K. 1995. Numerical modeling of the transient thermal interference of vertical U-tube heat exchangers. Ph.D. thesis, Texas A&M University, College Station.

Schaeffer, M. 1995. Computer simulation and experimental analysis of transport phenomena during the thermal processing of meat emulsion products. Ph.D. thesis, University of Wisconsin, Madison.

Thornton, J., et al. 1996. Residential vertical geothermal heat pump system models: Calibration to data. Madison, Wis.: Thermal Energy Specialists.